Anodic Stripping Voltammetry at a Hydrodynamic Mercury Electrode under High Mass Transport Conditions. 2. Experimental Verification of Theory and Implications for Sonovoltammetry

César Agra-Gutiérrez, Jon C. Ball, and Richard G. Compton*

Physical and Theoretical Chemistry Laboratory, Oxford University, South Parks Road, Oxford OX1 3QZ, United Kingdom

Received: May 15, 1998; In Final Form: June 26, 1998

Anodic stripping voltammetry experiments were carried out in aqueous lead solution using square wave voltammetry at insonated mercury thin film electrodes and compared to numerical theory developed in an earlier paper (Ball, J. C.; Compton, R. G. *J. Phys. Chem. B* **1998**, *102*, 3967). Excellent agreement was obtained under very fast mass transport conditions corresponding to the small (∼micrometer) diffusion layer thickness obtained under power ultrasound. The results provide further confirmation that the dominant contribution to the mass transport arises from diffusion layer thinning due to acoustic streaming except under extreme conditions. The choice of optimal square wave frequency under these conditions was investigated.

1. Introduction

Anodic stripping voltammetry (ASV) is commonly applied to the analytical determination of a wide range of trace metals and generally employs thin film mercury electrodes.[1,2] The method has two stages. First, a preconcentration step is applied in which electrodeposition of the target metal ion(s) in solution leads to the accumulation of metal in the (mercury) electrode, usually through the formation of an amalgam. Second, the electrode potential is swept positive, so inducing the oxidation of the metal(s) in the mercury film resulting in a characteristic voltammetric peak(s) that permits the determination of the target(s). The merits of using hydrodynamic conditions for the first or both stages of ASV include enhanced sensitivity and reproducibility in addition to the attractions of conducting the experiment under continuous flow conditions.[3−11] However, theory[12−15] has indicated that under conditions of merely modestly enhanced transport the associated reduction in the diffusion layer thickness can lead to significant deviations from the theory developed for conditions of semi-infinite diffusion.[16−19]

The simulation of linear sweep ASV has been carried out at uniformly accessible electrodes for both electrochemically reversible and quasi-reversible processes.[13,14] Such theory is approximately applicable to rotating disk and hanging mercury drop electrodes and possibly to insonated electrodes.[20] Theory has been extended to the case of channel[15] and "wall-jet"[12] electrodes. However, many applications of ASV are, in experimental practice, conducted using square wave voltammetry (SWV) since this offers many advantages as evaluated by Brett and Oliveira Brett:[21] speed of analysis, lower consumption of electroactive species, reduced problems with electrode passivation, and the possibility of conducting measurements without the need for the removal of dissolved oxygen.[22,23] In a previous paper[24] a theory for SWV as applied to electrochemically reversible processes undergoing anodic stripping has been developed for planar mercury electrodes. In addition SWV theory has been recently extended[25] to simulate simple irreversible reactions. The present paper seeks to compare the theory developed in the earlier paper[24] with experiments under conditions of high mass transport achieved by sonication with a view to assess the potential application of SWV in the presence of ultrasound.

2. Theory

We consider the electrode process

$$\mathrm{RED}_{(\mathrm{Hg})} - n\mathrm{e}^- \rightleftharpoons \mathrm{OX}_{(\mathrm{aq})}$$

corresponding to an ASV stripping peak in which the electrode potential is subjected to an anodic square wave voltammetric sweep (see ref 24). The time of pulse, t_p, is related to the frequency, f, of the pulse

$$t_p = \frac{1}{2f} \tag{1}$$

We next assume the electrode process to be electrochemically reversible such that the Nernst Equilibrium applies

$$\frac{[\mathrm{RED}]_{(\mathrm{Hg})}}{[\mathrm{OX}]_{(\mathrm{aq})}} = \exp\left[-\left(\frac{nF}{RT}\right)(E - E^{0\prime})\right] \tag{2}$$

where E is the potential on the square wave scan and $E^{0\prime}$ is the formal potential of the redox couple.

The pulse duration is typically very short, and film diffusion needs to be included in the model as suggested by the work of Osteryoung and co-workers.[26,27] To do this two separate equations are introduced. At the film surface the flux of RED and OX must be equal such that

$$D_R \left.\frac{\partial[\mathrm{RED}]}{\partial y}\right|_{y=0} = D_O \left.\frac{\partial[\mathrm{OX}]}{\partial y}\right|_{y=0} \tag{3}$$

where D_R is the diffusion coefficient of the reduced species within the film and y is the Cartesian coordinate perpendicular to the electrode surface. The transport within the film can be

* To whom correspondence should be sent.

S1089-5647(98)02247-0 CCC: $15.00
Published on Web 08/13/1998

assumed to be controlled by Fick's 2nd law of diffusion:

$$\frac{\partial[\mathrm{RED}]}{\partial t} = D_{\mathrm{R}}\frac{\partial^2[\mathrm{RED}]}{\partial y^2} \tag{4}$$

Finally, the transport of OX in solution is similarly controlled.

$$\frac{\partial[\mathrm{OX}]}{\partial t} = D_{\mathrm{O}}\frac{\partial^2[\mathrm{OX}]}{\partial y^2} \tag{5}$$

At the diffusion layer edge, $y = \delta$, the concentration of OX is set to $[OX]_{\mathrm{bulk}}$. We also assume that no intermetallic compounds are formed in the amalgam described above. A Cottrellian time grid is employed (see ref 24).

All programs were written in FORTRAN and executed on a Silicon Graphics Origin 2000 server. Results were analyzed using Microsoft Excel 7.0. The simulations were converged to 1%. Values used in computer simulation of the number of Cottrellian time nodes was 200; the number of real time nodes required for the same accuracy was 10 000; the number of solution spatial nodes was 8000, and the number of film spatial nodes 4000 was found to be appropriate (see ref 24 for definitions).

3. Experimental Section

The well-characterized and thermostated (25 ± 2 °C) electrochemical cell used for voltammetric and sonovoltammetric experiments has been described in detail previously.[28] The positioning of the working electrode in this cell is directly opposite the transducer probe and located near the cell bottom. The transducer probe to working electrode distance was 3 mm in all experiments reported below. The ultrasound generator employed was a VCX400 model sonic horn (Sonics and Materials, U.S.) equipped with a 13 mm titanium diameter probe emitting 20 kHz ultrasound. The sound intensity was varied between 0 and 40 W cm^{-2} as determined calorimetrically using the method suggested by Margulis.[29] All experiments were performed using a computer-controlled PGSTAT20 Autolab potentiostat (Eco-Chemie, Utrecht, Netherlands). The need for bipotentiometric[30] control of the titanium horn itself was eliminated by insulating the transducer from the probe with a thin Teflon disk and connecting the two with an insulating screw thread machined from Delrin instead of titanium. Thermostating of the cell (25 ± 2 °C) was accomplished by means of a glass cooling coil inserted in the solution through which water is circulated from a constant-temperature bath.

The working electrode consisted of a 2 mm copper electrode polished using diamond pastes of successively finer size down to 1 μm (Kemet, Kent, U.K.) which was then electrochemically coated with mercury following a procedure described in the literature.[31] Electroplating was carried out using a 0.01 M mercury(II) perchlorate and a 0.1 M perchloric acid solution at an applied potential of −0.6 V vs SCE where hydrogen evolution is not observed. This permitted the calculation of the thickness of the mercury film, which was 1 ±0.03 μm in all cases. This choice of substrate produces uniform mercury films that are not obtained on other electrode substrates such as platinum or glassy carbon where small mercury droplets are formed.[31,32] The films are also appropriate for using under sonication since they remain largely unaffected.[33] In addition, modeling of simple linear scan ASV of various metals using mercury-coated copper electrodes has shown[31] good correlation between theory and experiments in the case of Pb^{2+}. In this modeling no interactions were assumed to occur between copper and lead in the mercury film as required by the theory described above.

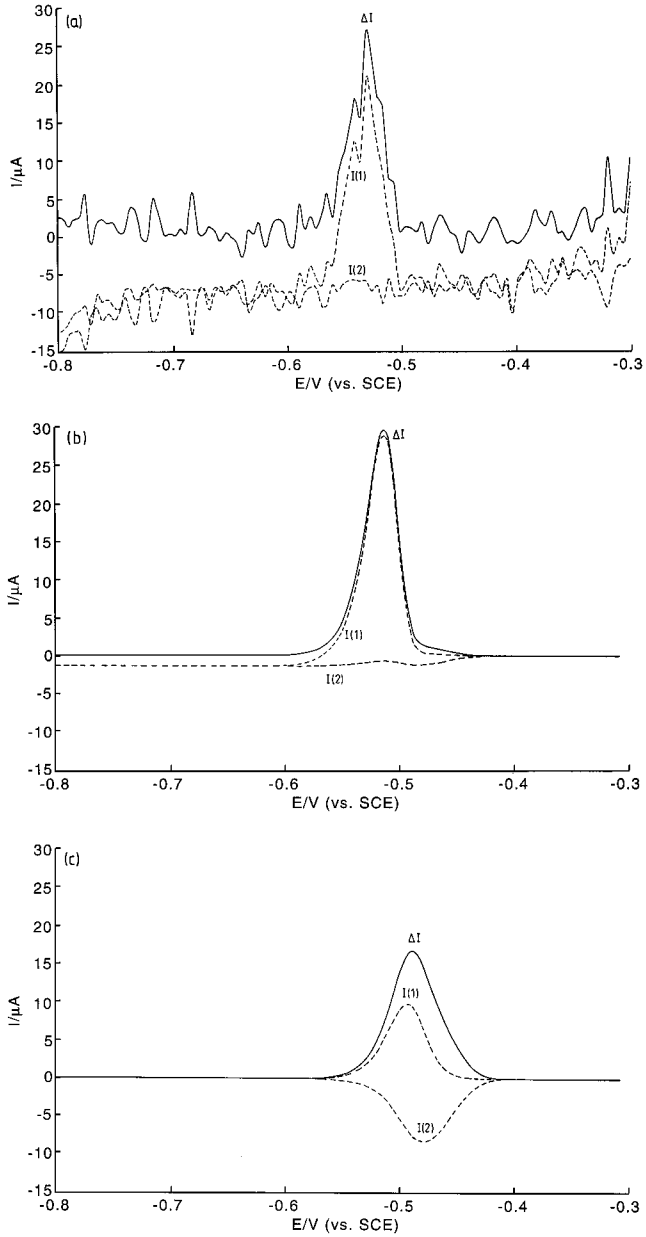

Figure 1. Square wave voltammograms for a frequency of 20 Hz obtained (a) experimentally in a 0.5 M NaCl, 0.1 M HCl, and 5 μM Pb^{2+} solution following a preconcentration time of 60 s at −0.8 V vs SCE using a 1 μm mercury film on copper under sonication of intensity 54 W cm^{-2} from a ultrasonic probe placed at 3 mm of the working electrode; (b) via simulation using a diffusion layer thickness of 2.4 μm; (c) via simulation under conditions of semi-infinite diffusion. Square wave parameters: pulse amplitude, $E_{\mathrm{SW}} = 25$ mV, and a step voltage, ΔE, of 5 mV.

Reagents used were of analytical grade or the highest commercially available purity. Hexaammineruthenium(III) chloride, mercury(II) perchlorate, perchloric acid, a lead(II) standard (0.483 mM), and a hydrochloric acid standard (0.974 M) were supplied by Aldrich and sodium chloride and potassium nitrate by BDH and were used as received. Solutions were prepared using UHQ grade water of resistivity not less than 18 MΩ cm (Elgastat, High Wycombe, Bucks, U.K.). All solutions were deaerated with pureshield argon prior to experiments.

The ASV procedure was a modified version of that described by Donten and Kublik.[31] Two hundred fifty milliliters of a

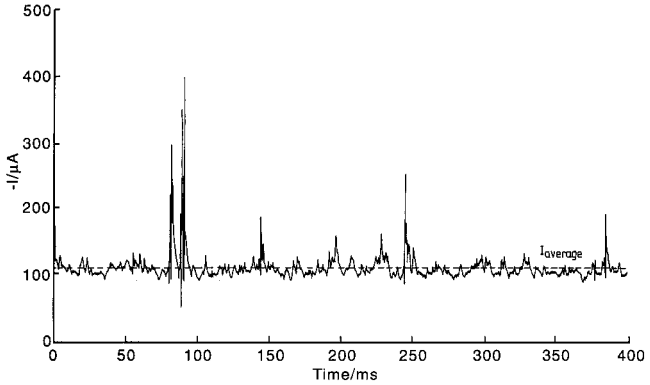

Figure 2. Time-resolved current signal for the reduction of 1 mM $Ru(NH_3)_6^{3+}$ in aqueous 0.1 M KNO_3 at an applied potential of −0.5 V vs SCE recorded in the presence of ultrasound of intensity 54 W cm^{-2} emitted from an ultrasonic probe placed at 3 mm from a 2 mm mercury-coated copper electrode.

solution containing 0.5 M NaCl, 0.1 M HCl, and 5 μM Pb^{2+} were placed in the sonoelectrochemical cell described above. The solution was then deaerated by purging with pureshield argon for 15 min while the electrode was held at −0.3 V vs SCE, where any lead present in the mercury film is stripped off while the film remains unaffected. The working electrode was then set at the deposition potential of −0.8 V vs SCE for 60 s. The anodic stripping voltammetry scan, square wave, was then started during which ultrasound was applied to the system as described above. Square wave parameters were amplitude 25 mV, step voltage of 5 mV, and frequencies varying between 20 and 1000 Hz. Time-resolved experiments were conducted in a solution containing 0.1 M KNO_3 and 1 mM $Ru(NH_3)_6Cl_3$ with the working electrode held at −0.5 V vs SCE where the mass-transport limited reduction current of $Ru(NH_3)_6^{3+}$ can be obtained to calibrate the diffusion layer thickness.[34]

4. Results and Discussion

In a previous paper,[24] a simulation approach to electrochemically reversible systems undergoing square wave voltammetry at hydrodynamic electrodes was developed. Significant deviations from semi-infinite diffusion theory were predicted for small diffusion layer thicknesses. Therefore, a series of experiments were carried out in which square wave voltammograms for a frequency of 20 Hz were obtained experimentally (Figure 1a) under applied ultrasound of intensity 54 W cm^{-2} emitted from a ultrasonic probe placed at 3 mm opposite a 2 mm mercury-coated copper electrode. The diffusion layer thickness under these conditions was calculated using eq 6 and the mass-transport-controlled current obtained during time-resolved experiments (shown in Figure 2) for the one-electron reduction of $Ru(NH_3)_6^{3+}$ in 0.1 M KNO_3 on a 2 mm mercury-coated copper electrode held at an applied potential of −0.5 V vs SCE (mass-transport-controlled current) under otherwise identical conditions of sonication.

$$I_{lim} = \frac{nFAD[Ox]}{\delta} \qquad (6)$$

I_{lim} is the limiting current, n the number of electrons involved, A the electrode area, 3.14 mm^2, F the Faraday constant, D the diffusion coefficient of the ruthenium(III) complex in water, 9.1×10^{-5} cm^2 s^{-1}, and [Ox] its concentration, 1 mM. A value of δ of 2.4 μm is obtained for an ultrasound intensity of 54 W cm^{-2} at a horn to electrode distance of 3 mm. Results (where ΔI is the difference between $I(1)$ and $I(2)$, the forward and backward currents during the square wave scan) were compared to the theoretical values predicted by the theory both under high mass-transport using the calculated value of δ reported above, Figure 1(b), and under conditions of semi-infinite diffusion, Figure 1(c). An excellent agreement is observed between experiment and the theoretical values predicted using the model of the "uniformly accessible electrode" for a diffusion layer thickness of 2.4 μm, parts a and b of Figure 1, respectively. Both differ considerably from the value predicted under conditions of semi-infinite diffusion. In particular, the magnitude and sign of $I(2)$ in Figure 1a correlate well with the predicted values. This observed behavior of $I(2)$ as the diffusion layer thickness decreases had been predicted by the theory and reported in a previous paper.[24] It was attributed to the fact that

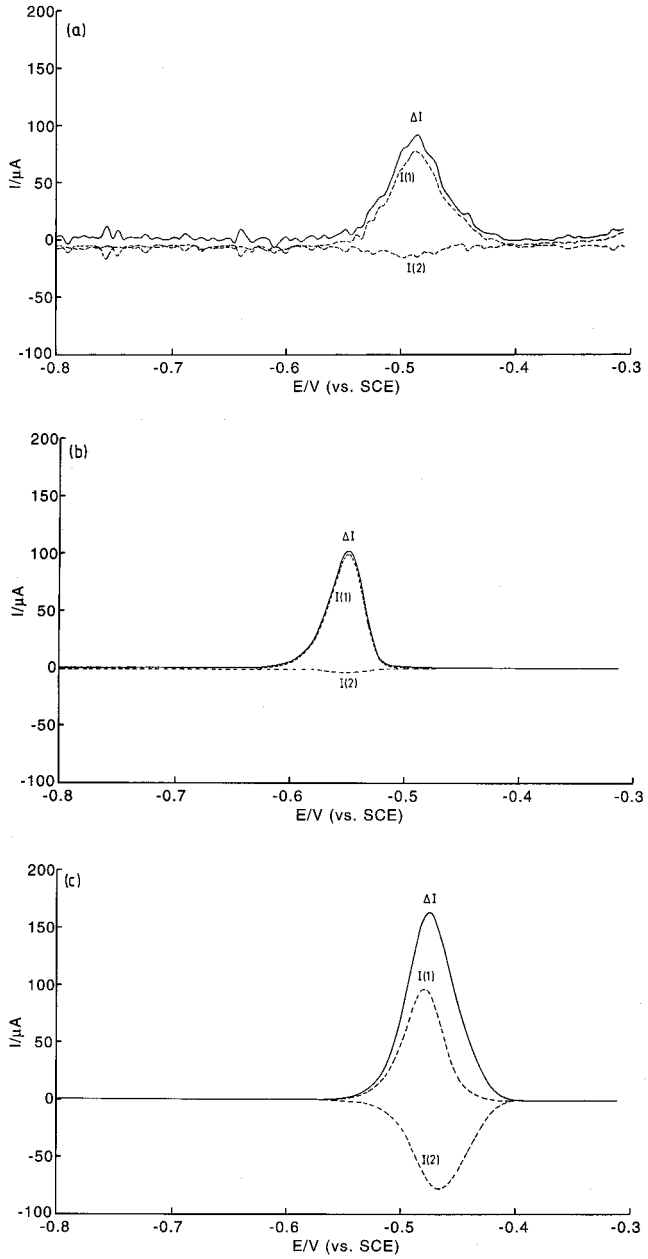

Figure 3. Square wave voltammograms for a frequency of 200 Hz obtained (a) experimentally in a 0.5 M NaCl, 0.1 M HCl and 5 μM Pb^{2+} solution following a preconcentration time of 60 s at −0.8 V vs SCE using a 1 μm mercury film on copper under sonication of intensity 54 W cm^{-2} from a ultrasonic probe placed at 3 mm of the working electrode; (b) via simulation for a diffusion layer thickness of 2.4 μm; (c) via simulation under conditions of semi-infinite diffusion. Other square wave parameters as in Figure 1.

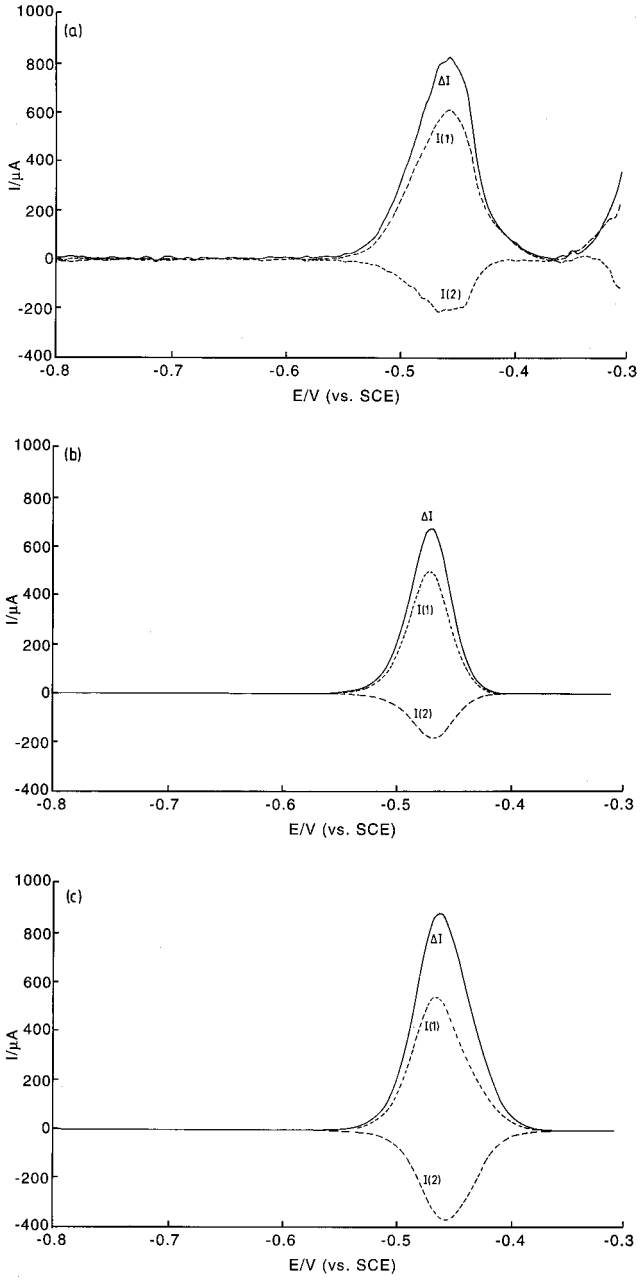

Figure 4. Square wave voltammograms for a frequency of 1000 Hz obtained (a) experimentally in a 0.5 M NaCl, 0.1 M HCl, and 5 μM Pb^{2+} solution following a preconcentration time of 60 s at −0.8 V vs SCE using a 1 μm mercury film on copper under sonication of intensity 54 W cm^{-2} from a ultrasonic probe placed at 3 mm of the working electrode; (b) via simulation using a diffusion layer thickness of 2.4 μm; (c) via simulation under conditions of semi-infinite diffusion. Other square wave parameters as in Figure 1.

at small diffusion layer thickness the pulse times studied $I(2)$ is sampled so late in comparison with the rate of diffusion of Pb^{2+} into the bulk of the solution that the Pb^{2+} released from the electrode in the forward-going pulse has been partially lost from the diffusion layer and cannot be reduced in the backward-going scan $I(2)$. It is worth pointing out that this strong agreement between theory and experiment occurs despite the strong cavitational events that occur under power ultrasound as shown by individual current spikes in Figure 2. Theory has been developed[34] that satisfactorily approximates the effect of ultrasound on the mass transport at the electrode surface by considering only the effect of "acoustic streaming" and by treating the system similar to related cases in hydrodynamic voltammetry as has been the case for the theory used in these simulations. Controversy still arises to identify the contribution of the underlying physical processes responsible for the huge increase in mass transport under insonation conditions. These include (i) acoustic streaming, (ii) jets caused by cavitational collapses, (iii) turbulent convection, (iv) microstreaming in the presence of oscillating bubbles, and (v) to some degree the fluctuating current density that might—owing to the calibration procedure—average to an apparent δ_{app} smaller than the geometric average. However, the present results are further evidence for a dominant effect of acoustic streaming on the mass transport at the electrode surface.

The effect of the frequency of the pulse can be observed in Figures 3 and 4, where square wave voltammograms obtained in the same conditions as those in Figure 1 are shown for the higher frequencies of 200 and 1000 Hz. As predicted by the theory (Figure 3b), $I(2)$ becomes slightly reductive as the pulse frequency is increased to 200 Hz. Further increase of the pulse frequency renders $I(2)$ more reductive. As discussed above experimental results obtained under power ultrasound deviate from simulation under conditions of semi-infinite diffusion and are best described using the "uniformly accessible electrode" model with a diffusion layer thickness of 2.4 μm. This observation can be explained along with the discussion provided above for the magnitude and sign of $I(2)$. As the frequency increases the Pb^{2+} released during the forward scan has less time to be diffuse away into the bulk of the solution and therefore is more readily available for reduction in the backward scan $I(2)$. The level of noise observed at SW frequencies of 200 and 1000 Hz (Figures 3a and 4b, respectively) is smaller than that obtained at 20 Hz and is attributed to transient cavitational effects occurring close to the electrode surface. These events are fast, as observed in Figure 2, and, therefore are likely to predominate at the slow current sampling rates obtained for lower SW frequencies.

5. Conclusions

The theory developed for SWV as applied to electrochemically reversible processes undergoing ASV at planar mercury electrodes has been corroborated with experiments in the presence of ultrasound. In particular, deviations from semi-infinite theory predicted under conditions of high mass transport correlated well with experiments in which small diffusion layer thicknesses were attained by the application of power ultrasound. These results provided further evidence for a dominant effect of "acoustic streaming" on the mass transport at the electrode surface. Finally, care should be taken when choosing the frequency in SWVASV experiments under small diffusion layer thicknesses since partial reduction of the metal ion species in the backward scan may be lost owing to diffusion of the metal ion species away from the electrode.

Acknowledgment. We thank the EPSRC for financial support through the Analytical Sciences Program (Grant No. GR/L/36413) and the EPSRC and BP Chemicals Ltd for a CASE studentship for J.C.B.

References and Notes

(1) Brainina, Kh.; Neyman, E. *Electroanalytical Stripping Methods*; John Wiley and Sons: New York, 1993.

(2) Wang, J. *Analytical Electrochemistry*; VCH: Weinheim, 1994.

(3) Batley, G. E.; Florence, T. M. *J. Electroanal. Chem.* **1974**, *55*, 23.

(4) Bakaanov, V. I.; Zakharov, M. S.; Antip'eva, V. A.; Grigorchenko, A. P. *Zh. Anal. Khim.* **1974**, *29*, 421.

(5) Brett, C. M. A.; Lima, J. L. F. C.; Quinaz Garcia, M. B. *Analyst* **1994**, *119*, 1229.
(6) Brett, C. M. A.; Neto, M. M. P. M. *J. Electroanal. Chem.* **1989**, *258*, 345.
(7) Brett, C. M. A.; Oliveira Brett, A. M.; Pereira, J. L. C. *Electroanalysis* **1991**, *3*, 83.
(8) Neto, M. M. P. M.; Rocha, M. M. G. S.; Brett, C. M. A. *Talanta* **1994**, *41*, 1597.
(9) Brett, C. M. A.; Quinaz Garcia, M. B.; Lima, J. L. F. C. *Electroanalysis* **1996**, *8*, 1169.
(10) Lieberman, S. H.; Zirino, A. *Anal. Chem.* **1974**, *46*, 20.
(11) Andrews, R. W.; Johnson, D. C. *Anal. Chem.* **1974**, *48*, 1057.
(12) Ball, J. C.; Compton, R. G.; Brett, C. M. A. *J. Phys. Chem*. **1998**, *102*, 162.
(13) Ball, J. C.; Compton, R. G. *Electroanalysis* **1997**, *9*, 765.
(14) Ball, J. C.; Compton, R. G. *Electroanalysis* **1997**, *9*, 1305.
(15) Ball, J. C.; Cooper, J. A.; Compton, R. G. *J. Electroanal. Chem.* **1997**, *435*, 229.
(16) Roe, D. K.; Toni, J. E. A. *Anal. Chem.* **1965**, *37*, 1503.
(17) Brett, C. M. A.; Oliveira Brett, A. M. *J. Electroanal. Chem.* **1989**, *262*, 83.
(18) Schiewe, J.; Oldham, K. B.; Myland, J. C.; Bond, A. M.; Vicente-Beckett, V. A.; Fletcher, S. *Anal. Chem.* **1997**, *69*, 2673.
(19) de Vries, W. T.; van Dalen, E. *J. Electroanal. Chem*. **1967**, *14*, 315.
(20) Compton, R. G.; Eklund, J. C.; Marken, F. *Electroanalysis* **1997**, *9*, 509.
(21) Brett, C. M. A.; Oliveira Brett, A. M. *Electrochemistry. Principles, Methods and Applications*; Oxford University Press: Oxford, U.K., 1993.
(22) Wojciechowski, M.; Go, W.; Osteryoung, J. *Anal. Chem.* **1985**, *57*, 155.
(23) Matysik, F.-M.; Matysik, S.; Oliveira Brett, A. M.; Brett, C. M. A. *Anal. Chem*. **1997**, *69*, 51.
(24) Ball, J. C.; Compton, R. G. *J. Phys. Chem*. **1998**, *102*, 3967.
(25) Fatouros, N.; Krulic, D. *J. Electroanal. Chem*. **1998**, *443*, 262.
(26) Kounaves, S. P.; O'Dea, J. J.; Chandresekhar, P.; Osteryoung, J. *Anal. Chem.* **1987**, *59*, 386.
(27) Kounaves, S. P.; O'Dea, J. J.; Chandresekhar, P.; Osteryoung, J. *Anal. Chem.* **1986**, *58*, 3199.
(28) Compton, R. G.; Eklund, J. C.; Page, S. D. *J. Phys. Chem*. **1995**, *99*, 4211.
(29) (a) Margulis, M. A.; Mal'tsev, A. N. *Russ. J. Phys. Chem*. **1969**, *43*, 592. (b) Mason, T. J.; Lorimer, J. P.; Bates, D. M. *Ultrasonics* **1992**, *30*, 40.
(30) Marken, F.; Compton, R. G. *Ultrason. Sonochem.* **1996**, *2*, S131.
(31) Donten, M.; Kublik, Z. *J. Electroanal. Chem*. **1985**, *196*, 275.
(32) Marken, F.; Rebbitt, T. O.; Booth, J.; Compton, R. G. *Electroanalysis* **1997**, *9*, 19.
(33) Agra-Gutiérrez, C.; Compton, R. G. *Electroanalysis* **1998**, *10*, 204.
(34) Marken, F.; Akkermans, R. P.; Compton, R. G. *J. Electroanal. Chem*. **1996**, *415*, 55.